

JointMotion: Joint Self-supervision for Joint Motion Prediction

Royden Wagner¹, Ömer Şahin Taş^{1,2}, Marvin Klemp¹, and Carlos Fernandez¹

¹ Karlsruhe Institute of Technology (KIT)

² FZI Research Center for Information Technology

Abstract. We present JointMotion, a self-supervised learning method for joint motion prediction in autonomous driving. Our method includes a scene-level objective connecting motion and environments, and an instance-level objective to refine learned representations. Our evaluations show that these objectives are complementary and outperform recent contrastive and autoencoding methods as pre-training for joint motion prediction. Furthermore, JointMotion adapts to all common types of environment representations used for motion prediction (i.e., agent-centric, scene-centric, and pairwise relative), and enables effective transfer learning between the Waymo Open Motion and the Argoverse 2 Forecasting datasets. Notably, our method improves the joint final displacement error of Wayformer, Scene Transformer, and HPTR by 3%, 7%, and 11%, respectively.

Keywords: Self-supervised learning · representation learning · multi-modal pre-training · motion prediction

1 Introduction

Self-supervised learning (SSL), where supervision signals are generated from unlabeled data, by design excels in applications with large amounts of unlabeled data and limited labeled data (e.g., [4, 8, 15]). Recently, SSL methods combined with supervised fine-tuning outperform plain supervised learning with the same amount of data [5, 16] and shorter training times [12]. This makes SSL a versatile choice to improve existing methods in a wide range of applications.

In this work, we focus on improving joint motion prediction for autonomous driving. Motion prediction aims to predict the future motion of traffic agents given their past motion and environment context, such as lane networks and traffic light states. Therefore, motion prediction is essential for estimating future interaction amongst traffic agents [6] and subsequently assessing the risk of planned trajectories [23]. The majority of recent motion prediction methods perform marginal prediction, where future motion is predicted for each agent individually (e.g., [21, 26, 31]). Joint motion prediction predicts scene-wide motion modes, i.e. a mode captures a joint set of future motion sequences for multiple agents within a traffic scene, enabling interaction modeling.

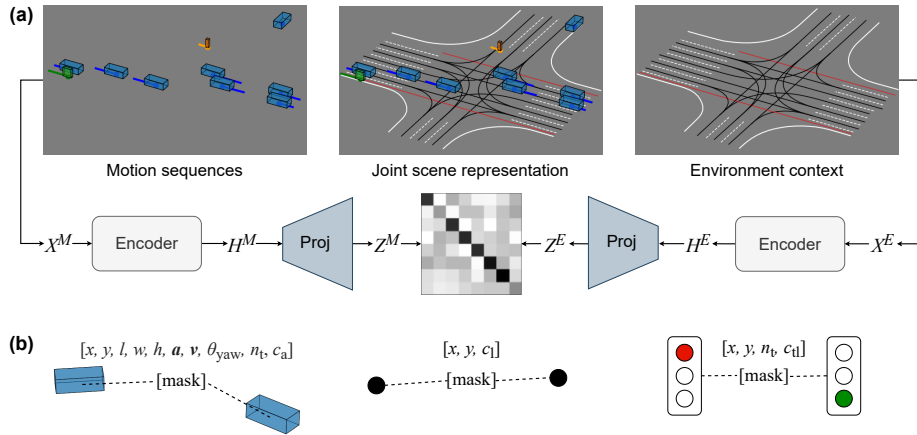


Fig. 1: JointMotion. (a) Connecting motion and environments: Our scene-level objective learns joint scene representations by matching embeddings of motion sequences (Z^M) and environment context (Z^E). (b) Masked instance modeling: Our instance-level objective includes a complete set of perception predictions: agent position (x, y), dimensions (l, w, h), acceleration (\mathbf{a}), velocity (\mathbf{v}), yaw angle (θ_{yaw}), temporal order (n_t), and class (c_a); lane node position (x, y) and class (c_l); traffic light position (x, y), temporal order (n_t), and class (c_{tl}).

Since joint motion prediction requires scene-wide representations, we propose a scene-level SSL objective connecting motion and environment. We complement this by an instance-level SSL objective that refines these representations, enhancing overall prediction accuracy. As scene-level objective, we match all past motion sequences in a scene to the corresponding environment context, such as map data and traffic light states. Thereby, a model learns which sets of motion sequences are likely in a given environment, including interaction amongst agents. As instance-level objective, we reconstruct masked motion sequences, masked lane polylines, and masked sequences of traffic light states. Unlike related work [7, 9], our instance-level objective includes a complete set of object features (agent dimensions, position, orientation, speed and acceleration profiles, and temporal order) to match to the environment context, rather than just positions. Hence, our main contributions are the two jointly optimized SSL objectives that accelerate the training and improve the precision of motion prediction models:

1. Connecting motion and environments via similarity learning, see Fig. 1 (a),
2. Masked instance modeling with a complete set of object features, see Fig. 1 (b).

2 Related work

SSL for motion prediction in autonomous driving. Inspired by the success of SSL in computer vision (e.g., [8, 15, 16]) and natural language processing

(e.g., [4, 24]), related methods apply SSL to pre-train motion prediction models for autonomous driving. PreTraM [33] learns a joint embedding space for trajectory and map data via contrastive learning. During pre-training, the similarity of trajectory and map embeddings from the same traffic scene is maximized, while the similarity to embeddings from other scenes is minimized (i.e., negative examples). This objective is misleading when similar scenes are sampled in a mini-batch, e.g., the map embeddings of two four-way stops should be similar, but are erroneously used as negative examples against each other. The concurrent works Traj-MAE [7], Forecast-MAE [9], and RMP [34] are masked autoencoding methods for pre-training motion prediction models. They mask trajectory and/or lane tokens and learn to reconstruct them. Traj-MAE and Forecast-MAE represent motion sequences as trajectory polylines, where each polyline point represents only the agents' position omitting available features such as velocity and acceleration profiles, agent dimensions, yaw angles, and temporal order (see Fig. 1 (b)). Furthermore, they do not include traffic light states as environment context. RMP limits the scope of pre-training to motion sequences and omits environment context, such as lane data and traffic light states, entirely. SSL-Lanes [3] extends lane masking with the objectives of distance to intersection prediction, maneuver and success/failure classification. Although these objectives are well adapted to motion prediction, they require non-trivial heuristics (e.g., for clustering maneuvers).

Joint motion prediction for autonomous driving. Joint motion predictions aims to predict the joint distribution of future motion sequences over multiple agents in a traffic scene. Thus, a predicted motion mode represents a scene-wide set of motion sequences with one sequence per agent. Scene Transformer [22] is an encoder-decoder transformer model for joint motion prediction. The encoder learns global scene-centric representations (i.e., agent, lane, and traffic light features), the decoder transforms these embeddings into joint motion modes. Global position embeddings are used for the learned scene-centric representations, which are more difficult to learn than pairwise relative position embeddings (cf. [10, 36]). MotionLM [25] reformulates motion prediction as language prediction task and learns a vocabulary of discrete motion vectors. Joint prediction modes are generated by jointly decoding sequences of motion vectors for multiple agents. MotionDiffuser [18] performs joint motion prediction as conditional denoising diffusion process. A scene-wide set of noisy trajectories (i.e., positions disturbed by Gaussian noise) is transformed by a denoiser into a scene-wide set of trajectories that approximates the ground truth joint prediction mode. The learned denoiser is conditioned on environment context such as lane data and traffic light states. At inference, trajectories are sampled from pure noise. Both MotionLM and MotionDiffuser use an agent-centric encoder [21], which leads to repeated computation since a traffic scene is encoded for each agent individually. To achieve a scene-wide context for a shared decoder, these methods concatenate multiple agent-centric embeddings with positional and rotation information into a common reference frame. Furthermore, their best per-

forming variants exhibit high inference latency and are not real-time capable (MotionLM: 250 ms³, MotionDiffuser: 409 ms).

Marginal motion prediction with auxiliary interactive prediction objectives. A marginal motion mode represents a single motion sequence for one agent. Many recent methods extend marginal prediction models with modules for interactive prediction objectives (i.e., dense [14, 27] or conditional prediction [20, 29]). In such methods, the prediction modules are still trained in a marginal manner, where training targets are marginal motion modes per agent. The additional modules are trained to combine marginal predictions by minimizing overlap between them. Thus, these methods do not learn to model scene-wide joint motion modes from ground up, but how to combine marginal modes with less overlap. This limits interaction modeling to the learned re-combination of marginal motion predictions.

3 Method

We present our method for self-supervised pre-training of motion prediction models in two steps. First, we describe our scene-level SSL objective (connecting motion and environments), then, we describe our agent-level SSL objective (masked instance modeling).

3.1 Connecting motion and environments

Joint motion prediction requires scene-wide representations to decode joint modes, which include predictions of multiple agents within a scene. Therefore, we propose pre-training motion prediction models by connecting motion and environments. This scene-level objective aims to learn a joint embedding space for motion sequences and environment context (see Fig. 1 (a)). Thus, a model implicitly learns which motion is likely in a given environment, including traffic rules and interaction amongst agents.

In detail, we use the past motion of all agents within a scene to generate a scene-level motion embedding (Z^M in Fig. 1) and combine lane data and traffic light states to a corresponding environment embedding (Z^E in Fig. 1). These embeddings are generated by modality-specific encoders (i.e., for motion, lanes, and traffic lights) followed by global average pooling and an MLP-based projector (Proj in Fig. 1). We perform average pooling on the intermediate embeddings (H^M and H^E in Fig. 1) to be invariant to variations in the number of agents and the complexity of environments. Following [13], we use two separate MLPs with LayerNorm and ReLU activations as projectors, each having a hidden dimension of 2048 and an output dimension of 256. We use the modality-specific encoders of recent motion prediction models (e.g., [22, 36]) without modifications and remove the additional projector after pre-training. The joint embedding space is learned

³ This latency is linearly interpolated, as inference latency is only reported up to the second best/largest model (see Table 8 in the Appendix of [25])

by similarity learning via redundancy reduction. Following [30, 35], we reduce the redundancy of vector elements per embedding (i.e., for Z^M and Z^E individually) and maximize their similarity by approximating the cross-correlation matrix of Z^M and Z^E to the corresponding identity matrix. The redundancy reduction term ensures that individual embedding elements capture different features. Therefore, it prevents model collapse with trivial solutions for all embeddings across all scenes (e.g., zero vectors). Non-trivial yet identical solutions are not explicitly prevented, but are unlikely, as empirically shown in [35]. In contrast to [33], our scene-level objective does not require negative examples, which are difficult to define in this context. Unlike [30], this objective maximizes the similarity of embeddings from different modalities (i.e., motion and environment) rather than augmented views of the same modality, removing the requirement to develop suitable augmentations.

3.2 Masked instance modeling

Scene-level representations are well suited to provide an overview of traffic scenes, but lack details at instance level. For example, the exact position of traffic agents in the past or lane curvatures. Therefore, we combine our scene-level objective with the instance-level objective of masked instance modeling to refine learned representations.

Inspired by masked sequence modeling [4, 16], we mask elements of past motion sequences, lane polylines, and past traffic light states and learn to reconstruct them from non-masked elements and environment context. As shown in Fig. 1, we represent traffic agents with 10 features rather than just past positions (cf. [7, 9]). In detail, we reconstruct agent positions (x, y), dimensions (l, w, h), acceleration (\mathbf{a}), velocity (\mathbf{v}), yaw angle (θ_{yaw}), temporal order (n_t), and classes (c_A , i.e., vehicles, cyclists, and pedestrians). For lanes, we reconstruct positions (x, y) and lane classes (c_L). For traffic light state sequences, we reconstruct positions (x, y), temporal order (n_t), and state classes (c_{TL} , i.e., green, yellow, and red). Following [36], positions, dimensions, accelerations, velocities, and yaw angles are represented as float values and temporal order and agent classes as boolean one-hot encodings.

For models that use late fusion mechanisms (e.g., [22, 36]), we use the modality-specific encoders to generate embeddings per modality (see Fig. 2 (a)). Afterwards, we concatenate these embeddings and use a shared local decoder to reconstruct masked sequence elements from non-masked elements and context from other modalities. As local decoder, we use transformer blocks with PreNorm, local attention [2] with an attention window of 32 tokens, 8 attention heads, rotary positional embeddings [28], and feed forward layers with an input and hidden dimension of 256 and 1024. For models that employ early fusion mechanisms (e.g., [21]), we use learned queries and a shared decoder to reconstruct the input sequences (see Fig. 2 (b)). Such models learn a compressed latent representation for multi-modal input. Therefore, we use learned queries in the same number as input tokens to decompress these representations and reconstruct the input sequences. We use a regular cross-attention mechanism between the learned

queries and compressed latent representations and a local self-attention mechanism within the set of learned queries. The resulting transformer blocks have the same hyperparameters as in the late fusion setup. For both variants, we use random attention masks for masking and a masking ratio 60%. As training target, we minimize the Huber loss between the reconstructed sequences (S^R) and the input sequences (S^I): $\mathcal{L}_{\text{recon}} = \lambda_A \mathcal{L}_A(S_A^R, S_A^I) + \lambda_L \mathcal{L}_L(S_L^R, S_L^I) + \lambda_{\text{TL}} \mathcal{L}_{\text{TL}}(S_{\text{TL}}^R, S_{\text{TL}}^I)$. If not specified otherwise, we set $\lambda_A = \lambda_L = \lambda_{\text{TL}} = 1$.

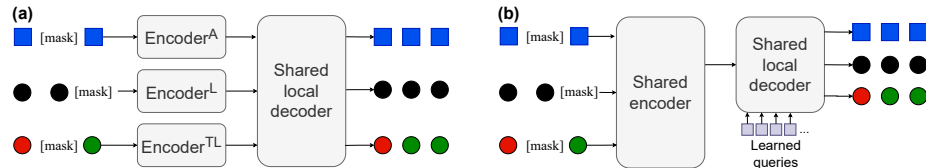


Fig. 2: Masked instance modeling with late and early fusion encoders. (a) Late fusion with modality-specific encoders for agents (Encoder^A), lanes (Encoder^L), and traffic lights (Encoder^{TL}). (b) Early fusion with a shared encoder for all modalities.

4 Experiments

4.1 Datasets and evaluation metrics

The Waymo Open Motion Dataset (WOMD) [11] is comprised of over 1.1 million data points extracted from 103,000 urban or suburban driving scenarios, spanning 20 seconds each. The state of object-agents includes attributes like position, dimensions, velocity, acceleration, orientation, angular velocity, and the status of turn signals. Each data point captures 1 second of past followed by 8 seconds of future data. We resample this time interval with 10Hz.

The Argoverse 2 Motion Forecasting Dataset (AV2) [32] is comprised of 250,000 urban or suburban driving scenarios each spanning 11 seconds, with 5 seconds of past and a 6 seconds of future data. The datasets entails interactions in over 2,000 km of roadways across six geographically diverse cities.

Evaluation metrics. Following [11], we use the mean average precision (mAP), the average displacement error (minADE), and the final displacement error (minFDE) to evaluate motion predictions. All metrics are computed using the minimum mode for $K = 6$ modes. Accordingly, the metrics for the mode closest to the ground truth are measured. We use the official challenge website to compute metrics on WOMD. For the AV2 dataset, we use the evaluation software provided by [36]. Therefore, joint modes (best scene-wide mode) are evaluated on the interactive splits and marginal modes (best mode for each agent individually) on the regular splits.

4.2 Comparison of self-supervised pre-training methods for joint motion prediction

In this experiment, we compare our method with recent self-supervised pre-training methods for autonomous driving using the WOMD dataset. Specifically, we compare with contrastive learning via PreTraM [33] and two masked autoencoding approaches, Forecast-MAE [9] and Traj-MAE [7].

Experimental setup. We pre-train and fine-tune well-established Scene Transformer [22] models on the WOMD training split. We use the publicly available implementation by [36] with 3 modality-specific encoders (i.e., for agents, lanes, and traffic lights) and a shared decoder for $K = 6$ motion modes. For pre-training, we add an shared local decoder for late fusion models (see Fig. 2) with 3 transformer blocks and the hyperparameters described in Sec. 3.2. For our method, we additionally add two projectors for scene-level representations as described in Sec. 3.1. For PreTraM, we follow its trajectory-map contrastive learning configuration and add two linear projection layers as projectors for trajectory and map embeddings. For Forecast-MAE, we use a masking ratio of 60% and reconstruct positions of lane polylines and past trajectories by minimizing the MSE loss. We exclude future trajectories, since self-supervised learning by design does not use the same labels as the intended downstream task (cf., [1]). For Traj-MAE, we use a masking ration of 60% and reconstruct positions of lane polylines and past trajectories by minimizing the corresponding Huber loss. For our method, we minimize the joint loss of our proposed objectives: $\mathcal{L}_{\text{JointMotion}} = \lambda_{\text{con}}\mathcal{L}_{\text{con}} + \mathcal{L}_{\text{recon}}$. We set $\lambda_{\text{con}} = 0.01$ and following [35] the weight of the redundancy reduction term $\lambda_{\text{red}} = 0.005$. We fine-tune the model using its joint configuration and hard loss assignment. Accordingly, the loss is computed for the best scene-wide joint prediction mode. As post-processing, we follow [19] and adjust the predicted confidences of redundant predictions. For all methods, we perform pre-training for 10 hours and fine-tuning for 23.5 hours using a training server with 4 A100 GPUs. For pre-training and fine-tuning, we use AdamW with an initial learning rate of 1e-4 and a step learning rate scheduler with a reduction rate of 0.5 and a step size of 25 epochs.

Results. Tab. 1 shows the results of this experiments. Explicit scene-level objectives (i.e., PreTraM and JointMotion) lead to better and more balanced performance across all agent types, while implicit scene-wide masked autoencoding with Forecast-MAE or Traj-MAE tends to focus more on the pedestrian class than on the others (see mAP scores). Therefore, it is likely that explicit scene-wide objectives enforce learning interactions between varying agent types more. Overall, our method achieves the best scores across all agent types. Our method without the objective of connecting motion and environments (JointMotion w/o CME), achieves worse performance. This shows that the combination of both objective works best and that the objectives are complementary. Fig. 3 shows the validation reconstruction losses of both configurations during pre-training and further highlights the complementary nature of our two objectives. Specifically, the reconstruction of past traffic light sequences and past motion are learned similar with both configurations. However, the lane reconstructions

are more accurate without our scene-level objective. We hypothesize that models pre-trained with our scene-level objective tend to focus more on the overall lane structure than on specific details of individual lane polylines.

Table 1: Comparison of self-supervised pre-training methods for joint motion prediction. All methods are used to pre-train Scene Transformer models [22] on the Waymo Open Motion dataset and evaluated on the validation split. Agent types: cyclist (cyc), pedestrian (ped), and vehicle (veh). “w/o CME” denotes our method without the objective of connecting motion and environments. Best scores are **bold**, second best are underlined.

Pre-training	mAP \uparrow				minADE \downarrow			minFDE \downarrow		
	avg	cyc	ped	veh	cyc	ped	veh	cyc	ped	veh
None	0.1596	0.1465	0.1821	0.1504	1.522	0.6982	1.486	3.653	1.654	3.476
Forecast-MAE [9]	0.1592	0.1420	0.1873	0.1482	1.529	0.6940	1.423	3.664	1.652	3.343
Traj-MAE [7]	0.1677	0.1492	0.1917	0.1623	1.421	0.7084	1.338	<u>3.320</u>	1.647	3.090
PreTraM [33]	0.1689	<u>0.1724</u>	0.1775	0.1569	1.488	0.7108	1.461	3.489	1.657	3.374
JointMotion w/o CME	<u>0.1784</u>	0.1652	<u>0.1903</u>	<u>0.1796</u>	<u>1.457</u>	<u>0.6996</u>	<u>1.317</u>	3.363	<u>1.630</u>	<u>3.033</u>
JointMotion	0.1940	0.1970	0.1964	0.1886	1.343	0.6767	1.288	3.095	1.583	2.941

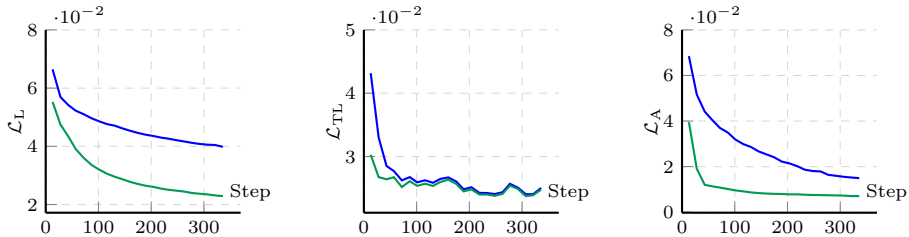


Fig. 3: Loss plots of complementary pre-training objectives. The green curve represents JointMotion w/o CME, while the blue curve represents JointMotion with the objective of connecting motion and environments. Consistent with the remainder of the document, L stands for lanes, TL stands for traffic lights, and A stands for agents.

Fig. 4 shows that Scene Transformer models pre-trained with our method achieve higher mAP scores on WOMD than models trained from scratch, even in the same total wall training time (pre-training + fine-tuning).

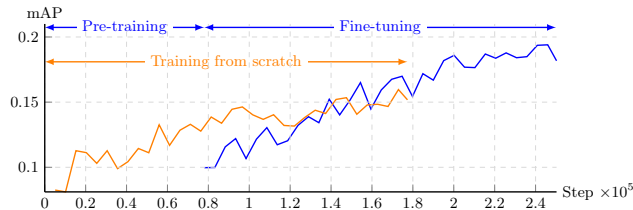


Fig. 4: Accelerating and improving training via SSL. Scene Transformer models pre-trained with JointMotion achieve higher mAP scores on WOMD than models trained from scratch, even in the same total wall training time (pre-training + fine-tuning).

5 Comparing scene-level self-supervision methods

In this experiment, we further compare the scene-level objectives PreTraM [33] and JointMotion. We train Scene Transformer, HPTR, and a joint configuration of Wayformer to cover all common types of environment representations in motion prediction (i.e., agent-centric, scene-centric, and pairwise relative).

Experimental setup. For Scene Transformer, we use the same configuration as in the previous experiment. For HPTR, we add 3 modality-specific encoders and use a shared decoder for $K = 6$ motion modes. For the joint configuration of Wayformer, we follow [18] and use a shared encoder for early fusion, which compresses the multi-modal input to 128 tokens. We concatenate multiple such agent-centric embeddings with positional and rotation information into a common reference frame and use a shared decoder to predict scene-wide joint modes. For pre-training the Wayformer model, we add our decoder for early fusion configurations (see Fig. 2). For all models, we employ the same optimizer and learning rate scheduling as in the previous experiment. All models are pre-trained for 10 hours and fine-tuned for 23.5 hours using a training server with 4 A100 GPUs. Evaluation is performed on the interactive validation split of WOMD and AV2. Our comparison is structured according to the performance metrics mAP (mean Average Precision), minSADE (minimum Social Average Displacement Error), minSFDE (minimum Social Final Displacement Error), MR (Miss Rate), and OR (Overlap Rate). minSADE measures the displacement error between the ground-truth future trajectories of interacting agents and the closest joint prediction out of a predefined set, averaged over the future time horizon [6]. This metric emphasizes the model’s ability to account for social interactions in predicting the average trajectory displacement accurately. On the other hand, minSFDE focuses on the displacement error at the time horizon endpoint.

Results. Table 2 shows the results of this experiment. Our method consistently outperforms PreTraM using different models with varying environment representations. Our method improves all models, while the improvement of the HPTR model (e.g., 11% lower minSFDE) is most significant and the improvement of the agent-centric Wayformer is least significant (e.g., 3% lower

minSFDE). The Wayformer model is not pre-trainable with PreTraM since an instance-level objective is required to decode the modality-specific tokens from fused representations (cf., Sec. 3.2). The lowest block shows that our method leads to transferable representations. Specifically, pre-training on WOMD improves fine-tuning on AV2.

Table 2: Comparing scene-level self-supervision methods. All metrics are computed using the Waymo Open Motion interactive (WOMD) and Argoverse 2 Forecasting (AV2) validation splits. Best scores are **bold**, second best are underlined.

Dataset	Pre-training	Model	mAP \uparrow	minSADE \downarrow	minSFDE \downarrow	MR \downarrow	OR \downarrow
WOMD	None	Scene Transformer	0.0822	<u>1.5255</u>	3.6715	<u>0.7372</u>	0.2868
	PreTraM [33]	Scene Transformer	0.0722	1.5415	<u>3.6508</u>	0.7385	0.2915
	JointMotion	Scene Transformer	0.0876	1.3830	3.2400	0.7090	0.2847
WOMD	None	HPTR	0.1033	1.1682	2.6003	0.6030	<u>0.2331</u>
	PreTraM [33]	HPTR	<u>0.1286</u>	<u>1.0981</u>	<u>2.5049</u>	<u>0.5863</u>	0.2345
	JointMotion	HPTR	0.1456	1.0564	2.4006	0.5591	0.2297
WOMD	None	Wayformer (joint)	0.1533	<u>1.0209</u>	2.3529	0.5461	0.2273
	JointMotion	Wayformer (joint)	0.1553	0.9939	2.2823	0.5270	0.2143
AV2	None	HPTR	<u>0.2554</u>	<u>2.255</u>	<u>1.138</u>	-	0.0988
	JointMotion WOMD	HPTR	0.2697	2.153	1.137	-	<u>0.1025</u>

6 Comparison with state-of-the-art methods for joint motion prediction

In this experiment, we compare our method with state-of-the-art methods for joint motion prediction in autonomous driving.

Experimental setup. We pre-train HPTR (configured as in Sec. 5) for 10 hours using JointMotion and fine-tune for 100 hours. We evaluate the methods in test and validation splits of WOMD. We use the official challenge website to compute performance metrics.

Results. Table 3 presents a comparative analysis of various state-of-the-art methods for joint motion prediction on interactive splits of WOMD. In the test split, we compare four different approaches. The Scene Transformer has a mAP of 0.1192 and is outperformed by the other methods in all metrics. GameFormer achieves a higher mAP of 0.1376 and exhibits competitive performance in terms of minSADE and minSFDE. MotionDiffuser and JointMotion (HPTR) are close contenders, with MotionDiffuser showing slightly better in all of the metrics compared to JointMotion (HPTR).

For the Validation split, the results are similar. GameFormer (joint) scores a mAP of 0.1339, with MotionLM (single replica) slightly outperforming it in terms of mAP, achieving 0.1687. JointMotion (HPTR) presents an improved mAP of 0.1761 compared to its counterparts. Following HPTR, we compare against single replica model of MotionLM and show its ensembling version for reference. MotionLM (ensemble) demonstrates superior overall performance, a result anticipated given power of ensembling.

Table 3: Comparison with state-of-the-art methods for joint motion prediction. All methods are evaluated on interactive splits of the Waymo Open Motion dataset. Following [36] we compare against single replica versions of joint prediction methods, ensemble versions are shown for reference. Best scores are **bold**, second best are underlined.

Split	Method (config)	Venue	mAP \uparrow	minSADE \downarrow	minSFDE \downarrow	MR \downarrow	OR \downarrow
Test	Scene Transformer (joint) [22]	ICLR'22	0.1192	0.9774	2.1892	0.4942	0.2067
	GameFormer (joint) [17]	ICCV'23	0.1376	0.9161	1.9373	<u>0.4531</u>	0.2112
	MotionDiffuser [18]	CVPR'23	0.1952	0.8642	<u>1.9482</u>	0.4300	0.2004
	JointMotion (HPTR)		<u>0.1869</u>	<u>0.9129</u>	2.0507	0.4763	<u>0.2037</u>
Val	GameFormer (joint) [17]	ICCV'23	0.1339	0.9133	1.9251	0.4564	-
	MotionLM (single replica) [25]	ICCV'23	<u>0.1687</u>	1.0345	2.3886	0.4943	-
	JointMotion (HPTR)		0.1761	<u>0.9689</u>	<u>2.2031</u>	<u>0.4915</u>	0.1990
	MotionLM (ensemble)	ICCV'23	0.2150	0.8831	1.9825	0.4092	-

7 Conclusion

In this work, we introduced a SSL method for joint motion prediction of all agents within a traffic scene. Our SSL framework integrates scene-level and agent-level objectives that operate complementarily, enhancing the training speed and accuracy of motion prediction models. Notably, our approach outperforms recent contrastive and autoencoding methods previously utilized for pre-training in motion prediction. Moreover, our objectives enable effective transfer learning between the Waymo Open Motion and the Argoverse 2 Forecasting datasets. Our evaluations demonstrate significant performance improvements over non-ensembling state-of-the-art joint prediction methods or joint-prediction variants of marginal-prediction architectures, underscoring the robustness and effectiveness of our proposed method.

References

1. Balestrieri, R., Ibrahim, M., Sobal, V., Morcos, A., Shekhar, S., Goldstein, T., Bordes, F., Bardes, A., Mialon, G., Tian, Y., et al.: A Cookbook of Self-Supervised Learning. arXiv:2304.12210 (2023) [7](#)
2. Beltagy, I., Peters, M.E., Cohan, A.: Longformer: The Long-Document Transformer. arXiv:2004.05150 (2020) [5](#)
3. Bhattacharyya, P., Huang, C., Czarnecki, K.: SSL-Lanes: Self-Supervised Learning for Motion Forecasting in Autonomous Driving. In: Conference on Robot Learning (CoRL) (2023) [3](#)
4. Brown, T., Mann, B., Ryder, N., Subbiah, M., Kaplan, J.D., Dhariwal, P., Neelakantan, A., Shyam, P., Sastry, G., Askell, A., et al.: Language Models are Few-Shot Learners. In: Advances in Neural Information Processing Systems (NeurIPS) (2020) [1](#), [3](#), [5](#)
5. Caron, M., Touvron, H., Misra, I., Jégou, H., Mairal, J., Bojanowski, P., Joulin, A.: Emerging Properties in Self-Supervised Vision Transformers. In: IEEE/CVF International Conference on Computer Vision (ICCV) (2021) [1](#)
6. Casas, S., Gulino, C., Suo, S., Luo, K., Liao, R., Urtasun, R.: Implicit Latent Variable Model for Scene-Consistent Motion Forecasting. In: European Conference on Computer Vision (ECCV) (2020) [1](#), [9](#)
7. Chen, H., Wang, J., Shao, K., Liu, F., Hao, J., Guan, C., Chen, G., Heng, P.A.: Traj-MAE: Masked Autoencoders for Trajectory Prediction. In: IEEE/CVF International Conference on Computer Vision (ICCV) (2023) [2](#), [3](#), [5](#), [7](#), [8](#)
8. Chen, T., Kornblith, S., Norouzi, M., Hinton, G.: A Simple Framework for Contrastive Learning of Visual Representations. In: International Conference on Machine Learning (ICML) (2020) [1](#), [2](#)
9. Cheng, J., Mei, X., Liu, M.: Forecast-MAE: Self-supervised Pre-training for Motion Forecasting with Masked Autoencoders. In: IEEE/CVF International Conference on Computer Vision (ICCV) (2023) [2](#), [3](#), [5](#), [7](#), [8](#)
10. Cui, A., Casas, S., Wong, K., Suo, S., Urtasun, R.: GoRela: Go Relative for Viewpoint-Invariant Motion Forecasting. In: IEEE International Conference on Robotics and Automation (ICRA) (2023) [3](#)
11. Ettinger, S., Cheng, S., Caine, B., Liu, C., Zhao, H., Pradhan, S., Chai, Y., Sapp, B., Qi, C.R., Zhou, Y., et al.: Large Scale Interactive Motion Forecasting for Autonomous Driving: The Waymo Open Motion Dataset. In: IEEE/CVF International Conference on Computer Vision (ICCV) (2021) [6](#)
12. Feichtenhofer, C., Li, Y., He, K., et al.: Masked Autoencoders As Spatiotemporal Learners. In: Advances in Neural Information Processing Systems (NeurIPS) (2022) [1](#)
13. Fini, E., Astolfi, P., Romero-Soriano, A., Verbeek, J., Drozdal, M.: Improved baselines for vision-language pre-training. Transactions on Machine Learning Research (2023) [4](#)
14. Gilles, T., Sabatini, S., Tsishkou, D., Stanculescu, B., Moutarde, F.: THOMAS: Trajectory Heatmap Output with learned Multi-Agent Sampling. In: International Conference on Learning Representations (ICLR) (2022) [4](#)
15. Grill, J.B., Strub, F., Altché, F., Tallec, C., Richemond, P., Buchatskaya, E., Doersch, C., Avila Pires, B., Guo, Z., Gheshlaghi Azar, M., et al.: Bootstrap Your Own Latent - A New Approach to Self-Supervised Learning. Advances in Neural Information Processing Systems (NeurIPS) (2020) [1](#), [2](#)

16. He, K., Chen, X., Xie, S., Li, Y., Dollár, P., Girshick, R.: Masked Autoencoders Are Scalable Vision Learners. In: IEEE/CVF Conference on Computer Vision and Pattern Recognition (CVPR) (2022) [1](#), [2](#), [5](#)
17. Huang, Z., Liu, H., Lv, C.: GameFormer: Game-theoretic Modeling and Learning of Transformer-based Interactive Prediction and Planning for Autonomous Driving. In: IEEE/CVF International Conference on Computer Vision (ICCV) (2023) [11](#)
18. Jiang, C., Cornman, A., Park, C., Sapp, B., Zhou, Y., Anguelov, D., et al.: MotionDiffuser: Controllable Multi-Agent Motion Prediction Using Diffusion. In: IEEE/CVF Conference on Computer Vision and Pattern Recognition (CVPR) (2023) [3](#), [9](#), [11](#)
19. Konev, S.: MPA: MultiPath++ Based Architecture for Motion Prediction. arXiv:2206.10041 (2022) [7](#)
20. Luo, W., Park, C., Cornman, A., Sapp, B., Anguelov, D.: JFP: Joint Future Prediction with Interactive Multi-Agent Modeling for Autonomous Driving. In: Conference on Robot Learning (CoRL) (2023) [4](#)
21. Nayakanti, N., Al-Rfou, R., Zhou, A., Goel, K., Refaat, K.S., Sapp, B.: Wayformer: Motion Forecasting via Simple & Efficient Attention Networks. In: IEEE International Conference on Robotics and Automation (ICRA) (2023) [1](#), [3](#), [5](#)
22. Ngiam, J., Caine, B., Vasudevan, V., Zhang, Z., Chiang, H.T.L., Ling, J., Roelofs, R., Bewley, A., Liu, C., Venugopal, A., et al.: Scene Transformer: A unified architecture for predicting multiple agent trajectories. In: International Conference on Learning Representations (ICLR) (2022) [3](#), [4](#), [5](#), [7](#), [8](#), [11](#)
23. Nishimura, H., Mercat, J., Wulfe, B., McAllister, R.T., Gaidon, A.: RAP: Risk-Aware Prediction for Robust Planning. In: Conference on Robot Learning (CoRL) (2023) [1](#)
24. Radford, A., Kim, J.W., Hallacy, C., Ramesh, A., Goh, G., Agarwal, S., Sastry, G., Askell, A., Mishkin, P., Clark, J., et al.: Learning Transferable Visual Models From Natural Language Supervision. In: International Conference on Machine Learning (ICML) (2021) [3](#)
25. Seff, A., Cera, B., Chen, D., Ng, M., Zhou, A., Nayakanti, N., Refaat, K.S., Al-Rfou, R., Sapp, B.: MotionLM: Multi-Agent Motion Forecasting as Language Modeling. In: IEEE/CVF International Conference on Computer Vision (ICCV) (2023) [3](#), [4](#), [11](#)
26. Shi, S., Jiang, L., Dai, D., Schiele, B.: Motion Transformer with Global Intention Localization and Local Movement Refinement. In: Advances in Neural Information Processing Systems (NeurIPS) (2022) [1](#)
27. Shi, S., Jiang, L., Dai, D., Schiele, B.: MTR++: Multi-Agent Motion Prediction with Symmetric Scene Modeling and Guided Intention Querying. IEEE Transactions on Pattern Analysis and Machine Intelligence pp. 1–16 (2024) [4](#)
28. Su, J., Lu, Y., Pan, S., Wen, B., Liu, Y.: RoFormer: Enhanced transformer with Rotary Position Embedding. Neurocomputing **568**, 127063 (2024) [5](#)
29. Sun, Q., Huang, X., Gu, J., Williams, B.C., Zhao, H.: M2I: From Factored Marginal Trajectory Prediction to Interactive Prediction. In: IEEE/CVF Conference on Computer Vision and Pattern Recognition (CVPR) (2022) [4](#)
30. Wagner, R., Taş, Ö.Ş., Klemp, M., Fernandez, C.: RedMotion: Motion Prediction via Redundancy Reduction. arXiv:2306.10840 (2023) [5](#)
31. Wang, X., Su, T., Da, F., Yang, X.: ProphNet: Efficient Agent-Centric Motion Forecasting With Anchor-Informed Proposals. In: IEEE/CVF Conference on Computer Vision and Pattern Recognition (CVPR) (2023) [1](#)

32. Wilson, B., Qi, W., Agarwal, T., Lambert, J., Singh, J., Khandelwal, S., Pan, B., Kumar, R., Hartnett, A., Pontes, J.K., et al.: Argoverse 2: Next Generation Datasets for Self-Driving Perception and Forecasting. arXiv:2301.00493 (2023) [6](#)
33. Xu, C., Li, T., Tang, C., Sun, L., Keutzer, K., Tomizuka, M., Fathi, A., Zhan, W.: PreTraM: Self-supervised Pre-training via Connecting Trajectory and Map. In: European Conference on Computer Vision (ECCV) (2022) [3](#), [5](#), [7](#), [8](#), [9](#), [10](#)
34. Yang, Y., Zhang, Q., Gilles, T., Batool, N., Folkesson, J.: RMP: A Random Mask Pretrain Framework for Motion Prediction. In: IEEE International Conference on Intelligent Transportation Systems (ITSC) (2023) [3](#)
35. Zbontar, J., Jing, L., Misra, I., LeCun, Y., Deny, S.: Barlow Twins: Self-Supervised Learning via Redundancy Reduction. In: International Conference on Machine Learning (ICML) (2021) [5](#), [7](#)
36. Zhang, Z., Liniger, A., Sakaridis, C., Yu, F., Van Gool, L.: Real-Time Motion Prediction via Heterogeneous Polyline Transformer with Relative Pose Encoding. In: Advances in Neural Information Processing Systems (NeurIPS) (2023) [3](#), [4](#), [5](#), [6](#), [7](#), [11](#)